DOI: 10.15826/chimtech.2019.6.3.01

Uma Dutta, Ariful Haque, Md. Motin Seikh*

Department of Chemistry, Visva-Bharati University, Santiniketan-731235, West Bengal, India
**E-mail: mdmotin.seikh@visva-bharati.ac.in*

Synthesis, structure and magnetic properties of Ti doped La_2MnNiO_6 double perovskite

We report sol-gel synthesis, structural characterization and magnetic properties of $La_2Mn_{1-x}Ti_xNiO_6$ ($0 \le x \le 1.0$). Ti doping removed the biphasic structure of La_2MnNiO_6 by suppression of rhombohedral structure and all the Ti containing samples crystallized in monoclinic $P2_1/n$ symmetry. La_2MnNiO_6 exhibits multiple magnetic transitions. The high temperature ferromagnetic transition of La_2MnNiO_6 gradually shifted to lower temperatures with increase in Ti doping. La_2TiNiO_6 ($x = 1.0$) does not show any long-range magnetic ordering. The suppression of magnetic transition by Ti doping is ascribed to the destruction of $Mn^{4+} – O – Ni^{2+}$ superexchange interaction. However, the signature of ferromagnetic phase persists up to 70% Ti doping, indicating the robustness of magnetic ordering in La_2MnNiO_6. These results suggest that the addition of Ti^{4+} truncates the ferromagnetic $Mn^{4+} – O – Ni^{2+}$ superexchange path and it likely promotes ferromagnetic cluster formation. The robustness of ferromagnetic state towards Ti substitution compared to the simple perovskite or spinel structure can be attributed to cationic ordering in double perovskite structure. Both the pure and Ti-doped samples exhibit magnetic frustration at lower temperatures due to partial cationic disordering. The absence of long-range ordering in La_2TiNiO_6, unlike La_2TiCoO_6 or Pr_2TiCoO_6, could be related to cationic disordering.

Keywords: double perovskite; ferromagnetic; superexchange interaction; magnetic frustration; cationic disorder; magnetic cluster.

Received: 20.08.2019. Accepted: 11.09.2019. Published: 15.10.2019.

© Uma Dutta, Ariful Haque, Md. Motin Seikh, 2019

Introduction

Oxides of transition metals with perovskite structure $LnMO_3$ (where Ln is rare earth elements or alkaline earth and M is transition element) exhibit various exotic physical properties related to the correlation between spin, charge, lattice and orbital degrees of freedom [1–3]. These strongly correlated electronic systems show competing electronic and magnetic states. Accordingly, compounds with perovskite structure have most extensively been studied by the physics and chemistry communities due to their magnetic, transport and magnetotransport properties [4]. Presence of second transition metal in the perovskite structure further improves the characteristic

features of the so-called double perovskites, $Ln_2MM'O_6$. The important features of double perovskite are cationic ordering, antiphase boundaries and multiple exchange interactions [5–7]. The rock salt ordering with alternate occupancy of octahedra by different metal ions takes place when there is a large size mismatch or the charge difference is greater than 2 [6, 8, 9]. All these are governed by the local electronic configuration of the transition metal ions. Extensive investigations on double perovskites reveal that by virtue of wide M/M' cationic range they exhibit multifunctional properties like insulating, metallic, ferromagnetic, magnetodielectric, multiferroic, etc., which are suitable for various technological applications [10–13].

Among the double perovskites, La_2MnNiO_6 has attracted special attention due to its striking properties such as multiple structures, multiple magnetic ground states, spin frustration and ferromagnetic insulating behaviour near room temperature with giant magnetodielectricity and magnetoresistance [14–19]. La_2MnNiO_6 is reported to crystallize in biphasic nature with rhombohedral ($R\bar{3}c$) and monoclinic ($P2_1/n$) [14, 15, 20–22] or rhombohedral and orthorhombic (*Pbnm*) symmetry [17, 23]. The high temperature synthesized sample is rhombohedral and low temperature one is monoclinic or orthorhombic, whereas for intermediate temperature range it is biphasic [23]. The phase fraction in the sample is also sensitive to the synthesis condition and post annealing treatment [14, 15, 18]. It was reported that the high-temperature phase transforms to $P2_1/n$ phase at low temperature [14]. The magnetic ordering temperatures are different for different phases. The $R\bar{3}c$ phase shows ferromagnetic ordering at relatively higher temperature (~280 K) compared to the $P2_1/n$ or *Pbnm* phase (~150 K) [16, 17]. The high temperature magnetic phase is governed by $Mn^{4+} - O - Ni^{2+}$, where for low temperature it is $Mn^{3+} - O - Ni^{3+}$ superexchange interactions [15–17, 23, 24]. There is also report on ferromagnetic transition at T_C~100 K in partially disordered sample, which was attributed to the $Mn^{3+} - O - Ni^{3+}$ interaction [15]. Furthermore, there is also appearance of spin glass behaviour in La_2MnNiO_6 associated with the competing interaction between ferromagnetic superexchange and disorder induced antiferromagnetic $Mn^{4+} - O - Mn^{4+}$ and $Ni^{2+} - O - Ni^{2+}$ interactions [15, 18, 25]. This suggests that the cationic disordering suppressed the high temperature ferromagnetic $Mn^{4+} - O - Ni^{2+}$ interaction of perfectly ordered phase. Another extensively studied compound is La_2MnCoO_6 with ferromagnetic T_C~230 K [26]. The double perovskites in which both metal ions are magnetic exhibit ferromagnetic ordering. However, for the ordered perovskite with single magnetic ion the long-range magnetic ordering is antiferromagnetic and the interaction is supersuperexchange with separation of magnetic centres larger than 5 Å [27, 28]. Such interaction also becomes weaker as reflected from the ordering temperatures. The observed T_N values for La_2CoTiO_6 and Pr_2CoTiO_6 are respectively, 15 K and 17 K [28, 29]. Thus, it would be interesting to investigate the ferromagnetic to antiferromagnetic crossover starting from an ordered ferromagnetic system by gradual replacing one magnetic ion by a nonmagnetic one.

In the present studies we have gradually replaced Mn^{4+} in La_2MnNiO_6 by Ti^{4+} to better understand the role of Mn^{4+} in determining the structural and magnetic properties. To the best of our knowledge there is no report in the literature on in-

vestigation of Ti doping in La_2MnNiO_6. The ionic radius of Ti^{4+} (0.605 Å) is larger than that for Mn^{4+} (0.530 Å) [30]. In addition, there are other aspects of this substitution. The replacement of magnetic Mn^{4+} by nonmagnetic Ti^{4+} will make magnetic dilution in system, which in turn will truncate the ferromagnetic exchange path. Thus, substitution of Ti^{4+} in La_2MnNiO_6 is expected to rapidly destroy the ferromagnetic state. Furthermore, by considering the retention of cationic ordering it will bring antiferromagnetic supersuper-exchange $Ni^{2+} - O - Ti^{4+} - O - Ni^{2+}$ in place of ferromagnetic $Ni^{2+} - O - Mn^{4+} - O - Ni^{2+}$ exchange path. We observed that the ferromagnetic ground state of La_2MnNiO_6 is very robust and it persists up to 70% doping of Ti^{4+}. We did not observe any antiferromagnetic ordering in La_2TiNiO_6 could be due to cationic disordering.

Experimental

Polycrystalline $La_2Mn_{1-x}Ti_xNiO_6$ ($0 \le x \le 1$) samples were prepared by modified sol-gel technique. At first, stoichiometric amounts of metal nitrates (La, Ni) and acetate (Mn) were dissolved in 100 ml double distilled water followed by the addition of about 5 ml concentrated nitric acid to prevent the hydrolysis of the aquated metal ions. In another small beaker stoichiometric amount (1:1) of titanium isopropoxide [$Ti\{OCH(CH_3)_2\}_4$], and acetyl acetone were mixed and stirred for about several minutes. These two different solutions were mixed in one single beaker and were stirred for about one hour using a magnetic stirrer to get a clear solution. Citric acid was then added to the solution at four times mole ratio of the total metal ions. The final pH of the solution was found to be ~2. The resulting solution was stirred overnight followed by evaporation of solvent at 100 °C to obtain the gel. The obtained gel was dried by increasing the temperature of hotplate to 150 °C to transform the gel into crude precursor. The crude powders were ground thoroughly by using an agate mortar-pestle and calcined at 500 °C for 6 h in air. The final calcination was performed at 700 °C for 6 h in air to achieve the pure phase samples.

The powder X-ray diffraction (PXRD) patterns were registered with a Bruker D8 Advance X-ray diffractometer using Cu Kα radiation (λ = 1.5418 Å) operating at 40 kV and 40 mA. The PXRD patterns were recorded in the 2θ range of 10–120° using Lynxeye detector (1D mode) with a step size of 0.02° and a dwell time of 1s per step. Iodometric titration of the samples confirms the oxygen stoichiometry fixed to "O_6" within the limit of accuracy ±0.05.

The dc magnetization measurements were performed using a superconducting quantum interference device (SQUID) magnetometer with a variable temperature cryostat (Quantum Design, San Diego, USA). The magnetic ac susceptibility, $\chi_{ac}(T)$ was measured with a PPMS (Quantum Design, San Diego, USA) with the frequency ranging from 10 Hz to 10 kHz. All the magnetic measurements were performed on powder samples putting inside a Teflon capsule.

Results and discussion

The PXRD patterns for all the $La_2Mn_{1-x}Ti_xNiO_6$ (x = 0, 0.2, 0.3, 0.5, 0.7 and 1.0) samples recorded in the 2q-range 10–120° are shown in Fig. 1. All the pat-

terns are refined by Rietveld method using FullProf suit program [31]. The pattern of the parent compound ($x = 0$) La_2MnNiO_6 can only be refined properly by considering a mixed rhombohedral $R\bar{3}c$ and monoclinic $P2_1/n$ phases. The biphasic nature composed of rhombohedral and monoclinic phases for La_2MnNiO_6 sample was reported in the literature by several researchers [14, 15, 18, 32]. However, the phase fraction depends on synthesis condition as well as on post-synthesis annealing treatment. We observed predominant monoclinic phase (80%) over rhombohedral (20%) one for the sol-gel synthesized La_2MnNiO_6 with final heat treatment in air at 700 °C for 6 h. However, all the Ti doped samples can be nicely indexed with monoclinic structure (sp. gr. $P2_1/n$) (Fig. 1). Thus, the Ti doping suppressed the rhombohedral phase of La_2MnNiO_6. The detailed structural and refinement parameters are given in Table 1. From the Table, one can see the systematic increase in cell volume with the increase in Ti^{4+} content as expected for its larger ionic radius compared to that of Mn^{4+} [30]. We observed that the size of NiO_6 octahedra are slightly larger than that of MnO_6 as reported in the literature [33].

Fig. 2 shows the temperature dependent dc-magnetization measured in both the zero field-cooled (ZFC) and field-cooled (FC) protocols under an applied magnetic field of 500 Oe for the temperature range 5–300 K. The magnetization data of $x = 0$ parent phase exhibit ferromagnetic transition (T_C~280 K) just below room temperature (Fig. 2, *a*). One should notice the large thermomagnetic irreversibility between ZFC and FC data branch immediate below T_C~280 K, where ZFC data show a hump. The ZFC data also

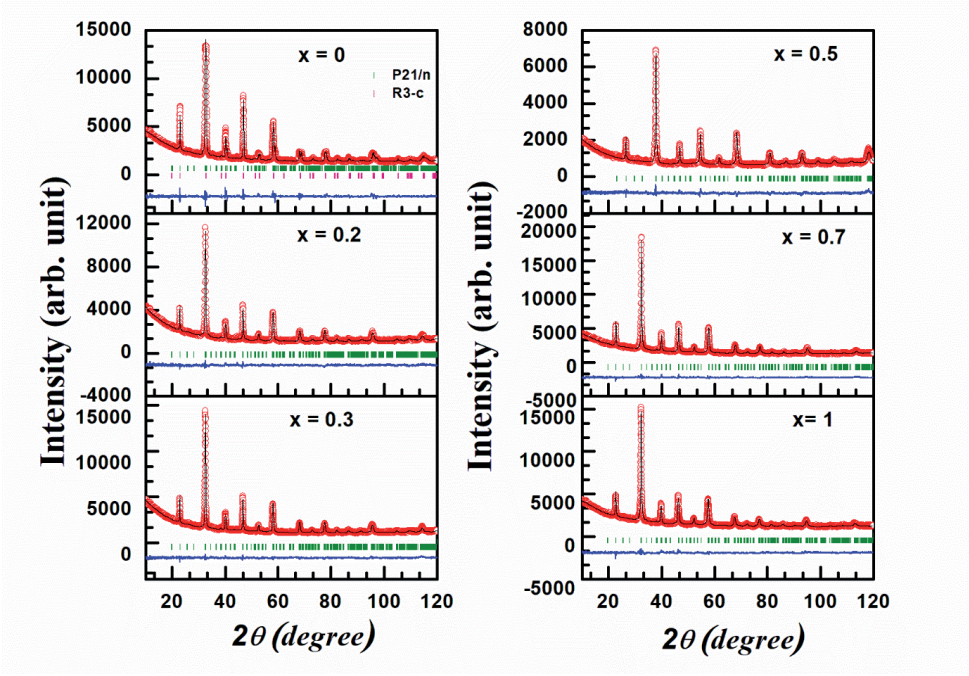

Fig. 1. Powder X-ray diffraction patterns of $La_2Mn_{1-x}Ti_xNiO_6$ ($x = 0$, 0.2, 0.3, 0.5, 0.7 and 1.0). The open red circles, black lines, the bottom blue lines and vertical bars represent the experimental data, calculated pattern, difference curve and Bragg position, respectively

Table 1

Structural refinement parameters for $Ln_2Mn_{1-x}Ti_xNiO_6$ ($0 \le x \le 1$) ceramics

	$x = 0$		$x = 0.2$	$x = 0.3$	$x = 0.5$	$x = 0.7$	$x = 1$
	$P2_1/n$	$R\bar{3}c$					
a (Å)	5.471 (4)	5.516 (2)	5.483 (9)	5.490 (8)	5.511 (8)	5.524 (5)	5.542 (6)
b (Å)	5.493 (3)	5.516 (1)	5.506 (4)	5.513 (6)	5.527 (2)	5.538 (6)	5.553 (6)
c (Å)	7.742 (4)	13.237 (7)	7.760 (4)	7.767 (4)	7.783 (7)	7.802 (5)	7.821 (6)
V (Å^3)	232.72	348.78	234.342	235.156	237.110	238.745	240.778
β (°)	89.369	γ = 120	89.540	89.719	89.720	90.197	90.244
R_B (%)	10.4		13.6	10.8	11.9	9.20	12.3
R_f (%)	14.5		22	23.4	17.0	24.4	26.8
χ^2	2.97		2.63	2.38	2.28	2.26	2.30
Bond length	2×Mn—O_1: 1.930 Å 2×Mn—O_2: 1.875 Å 2×Mn—O_3: 1.956 Å 2×Ni—O_1: 1.991 Å 2×Ni—O_2: 2.037 Å 2×Ni—O_3: 2.007 Å La—O1: 2.318 Å	Mn1—O_1: 1.899 Å Ni2—O_1: 2.029 Å La1—O1: 3×2.453 Å 6×3.056 Å 3×2.771 Å	×Mn/Ti—O_1: 1.934 Å 2×Mn/Ti—O_2: 1.885 Å 2×Mn/Ti—O_3: 1.906 Å 2×Ni—O_1: 2.023 Å 2×Ni—O_2: 2.046 Å 2×Ni—O_3: 2.033 Å	2×Mn/Ti—O_1: 1.935 Å 2×Mn/Ti—O_2: 1.888 Å 2×Mn/Ti—O_3: 1.909 Å 2×Ni—O_1: 2.019 Å 2×Ni—O_2: 2.048 Å 2×Ni—O_3: 2.035 Å	2×Mn/Ti—O_1: 1.939 Å 2×Mn/Ti—O_2: 1.894 Å 2×Mn/Ti—O_3: 1.914 Å 2×Ni—O_1: 2.023 Å 2×Ni—O_2: 2.054 Å 2×Ni—O_3: 2.041 Å	×Mn/Ti—O_1: 1.941 Å 2×Mn/Ti—O_2: 1.899 Å 2×Mn/Ti—O_3: 1.920 Å 2×Ni—O_1: 2.031 Å 2×Ni—O_2: 2.058 Å 2×Ni—O_3: 2.044 Å	2×Ti—O_1: 1.946 Å 2×Ti—O_2: 1.905 Å 2×Ti—O_3: 1.926 Å 2×Ni—O_1: 2.037 Å 2×Ni—O_2: 2.064 Å 2×Ni—O_3: 2.050 Å

Continuation of table

	$x = 0$		$x = 0.2$	$x = 0.3$	$x = 0.5$	$x = 0.7$	$x = 1$
	$P2_1/n$	$R\bar{3}c$					
	La—O_1: 3.121 Å La—O_1: 2.723 Å La—O_1: 2.829 Å La—O_2: 2.787 Å La—O_2: 2.729 Å La—O_2: 3.010 Å La—O_2: 2.463 Å La—O_3: 2.713 Å La—O_3: 2.455 Å La—O_3: 2.767 Å La—O_3: 3.057 Å		2La—O_1: 2.338 Å La—O_1: 2.721 Å La—O_1: 2.826 Å La—O_1: 3.148 Å La—O_2: 2.476 Å La—O_2: 2.733 Å La—O_2: 2.792 Å La—O_2: 3.024 Å La—O_3: 2.459 Å La—O_3: 2.727 Å La—O_3: 2.780 Å La—O_3: 3.063 Å	La—O_1: 2.341 Å La—O_1: 2.725 Å La—O_1: 2.830 Å La—O_1: 3.152 Å La—O_2: 2.480 Å La—O_2: 2.735 Å La—O_2: 2.793 Å La—O_2: 3.029 Å La—O_3: 2.460 Å La—O_3: 2.732 Å La—O_3: 2.784 Å La—O_3: 3.064 Å	La—O_1: 2.349 Å La—O_1: 2.732 Å La—O_1: 2.838 Å La—O_1: 3.163 Å La—O_2: 2.487 Å La—O_2: 2.742 Å La—O_2: 2.800 Å La—O_2: 3.037 Å La—O_3: 2.467 Å La—O_3: 2.739 Å La—O_3: 2.791 Å La—O_3: 3.072 Å	2La—O_1: 2.355 Å La—O_1: 2.737 Å La—O_1: 2.843 Å La—O_1: 3.172 Å La—O_2: 2.500 Å La—O_2: 2.741 Å La—O_2: 2.798 Å La—O_2: 3.052 Å La—O_3: 2.465 Å La—O_3: 2.754 Å La—O_3: 2.805 Å La—O_3: 3.070 Å	La—O_1: 2.367 Å La—O_1: 2.745 Å La—O_1: 2.851 Å La—O_1: 3.182 Å La—O_2: 2.508 Å La—O_2: 2.748 Å La—O_2: 2.805 Å La—O_2: 3.061 Å La—O_3: 2.472 Å La—O_3: 2.762 Å La—O_3: 2.813 Å La—O_3: 3.078 Å
Bond angle (°)	Mn—O_1—Ni: 158.44 Mn—O_2—Ni: 161.16 Mn—O_3—Ni: 162.62	Mn—O—Ni: 162.67	Mn—O_1—Ni: 158.31 Mn—O_2—Ni: 162.61 Mn—O_3—Ni: 161.20	Mn—O_1—Ni: 158.3 Mn—O_2—Ni: 162.6 Mn—O_3—Ni: 161.21	Mn—O_1—Ni: 158.26 Mn—O_2—Ni: 162.62 Mn—O_3—Ni: 161.22	Mn—O_1—Ni: 158.27 Mn—O_2—Ni: 162.57 Mn—O_3—Ni: 161.27	Mn—O_1—Ni: 158.25 Mn—O_2—Ni: 162.57 Mn—O_3—Ni: 161.28

show a second broad hump at low temperature centred around 25 K. Below T_C, FC data show a plateau followed by a definite slope change below 100 K (Fig. 2, *a*). Such magnetic behaviour of the parent phase is in good agreement with the reported data which supports the prevalence three magnetic phases in the temperature window 5–300 K [15–17, 23, 24]. The high temperature T_C is associated with the ferromagnetic $Mn^{4+} - O - Ni^{2+}$ superexchange interaction of cation ordered state. The transition below 100 K ascribed to the $Mn^{3+} - O - Ni^{3+}$ superexchange interaction and lowest temperature anomaly was attributed to the magnetic frustration arising out of partial cationic disordering [15, 18, 25]

For the Ti doped sample with $x = 0.2$, the high temperature magnetic transition

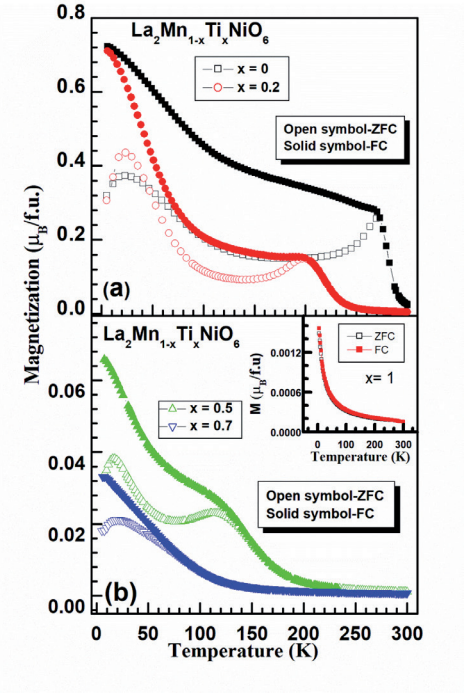

Fig. 2. Temperature dependent dc-magnetization of $La_2Mn_{1-x}Ti_xNiO_6$: *a* — for $x = 0$ and 0.2 and (*b*) for $x = 0.5$ and 0.7. Inset in (*b*) shows the data for La_2TiNiO_6

largely shifted (~60 K) to lower temperature at T_C~220 K (Fig. 2, *a*). However, the shape of the curve remains similar to that of the parent phase, though the thermomagnetic hysteresis loop shrinks compared to the $x = 0$ sample (Fig. 2, *a*). However, the upturn in magnetization below 100 K is not much shifted for $x = 0.2$ sample compared to $x = 0$. This result indicates that the high temperature magnetic transition associated with $Mn^{4+} - O - Ni^{2+}$ superexchange interaction is largely hampered compared to the $Mn^{3+} - O - Ni^{3+}$ superexchange interaction. This could be due to preferential isovalent substitution effect. Thus, it can be suggested that for 20% Ti doped sample the cationic ordering persists. For $x = 0.5$ the T_C value comes down to 150 K and still one can observe the double humps in ZFC branch data, upturn in FC data below 50 K as well as the thermomagnetic irreversibility (Fig. 2, *b*). It is worth mentioning that the parent phase sample with orthorhombic *Pbnm* or monoclinic $P2_1/n$ structures exhibits ferromagnetic transition at T_C~150 K ascribed to the $Mn^{3+} - O - Ni^{3+}$ superexchange interaction [15–17, 24]. However, we believe that the T_C~150 K for $x = 0.5$ sample is not associated with $Mn^{3+} - O - Ni^{3+}$ superexchange interaction like in parent phase, rather it is related to the weakening of $Mn^{4+} - O - Ni^{2+}$ superexchange interaction due to substitution of nonmagnetic Ti^{4+} in place of Mn^{4+}. The second magnetic phase further shifted below 50 K as indicated by the upturn in FC data in $x = 0.5$ sample (Fig. 2, *b*). This indicates that still there is possible cationic ordering up to 50% Ti doping in La_2MnNiO_6. On further increase in Ti doping to $x = 0.7$, there is only one broad hump in ZFC data around 20 K and FC data show up turn below 100 K (Fig. 2, *b*). This indicates that the high and

low temperature transitions as well as low temperature magnetic frustration merged together. For complete substitution of Mn by Ti i.e. $x = 1.0$ sample does not show any anomaly in the magnetization data and ZFC-FC superimposed as shown in inset of Fig. 2, *b*. This behaviour is typical for a paramagnetic material. This suggests that La_2TiNiO_6 does not show any kind of long-range ordering.

The gradual change in magnetic properties with replacement of magnetic Mn^{4+} by nonmagnetic Ti^{4+} in La_2MnNiO_6 is also supported from the isothermal magnetization data measured at 5 K under an applied field of ±5 T (Fig. 3). There is also a systematic decrease in magnetization as expected for magnetic dilution, but all the samples up to $x = 0.7$ exhibit clear hysteresis loop suggesting the prevalence of ferromagnetic component in the system. However, the opening of the loop is small as reported for the parent phase [15, 24]. There is no hysteresis loop for $x = 1.0$ sample (see inset in Fig. 3) which practically shows a linear increase in magnetization with field as expected for a paramagnet (see inset in Fig. 3).

Let us discuss the observed change in magnetization in $La_2Mn_{1-x}Ti_xNiO_6$. The substitution of Mn^{4+} by nonmagnetic Ti^{4+} will truncate the ferromagnetic $Ni^{2+} - O - Mn^{4+} - O - Ni^{2+}$ superexchange path to $Ni^{2+} - O - Ti^{4+} - O - Ni^{2+}$. This doping not only destroy the ferromagnetic exchange path, but also results in weak antiferromagnetic interaction between the Ni^{2+} cation. The weak antiferromagnetic interaction between Ni^{2+} takes place via super superexchage interaction mediated through $O - Ti^{4+} - O$ linker. This type of antiferromagnetic interaction is observed in half doped $LaNi_{0.5}Al_{0.5}O_3$ through $Ni - O - Al - O - Ni$ exchange path [34]. Thus, with increase in Ti doping the ferromagnetism in La_2MnNiO_6 becomes more and more weaker as reflected by the change in T_C shown in Fig. 4. This result is very contrasting with the effect of Ti doping in single perovskite manganite $Sm_{0.55}Sr_{0.45}MnO_3$, where just 4% of Ti doping leads for disappearing of the ferromagnetic state [35]. The robustness of ferromagnetism towards magnetic dilution in double perovskite La_2MnNiO_6 may be related to the cationic ordering. Most likely the disruption of $Ni^{2+} - O - Mn^{4+} - O - Ni^{2+}$ superexchange path leads to fragmented

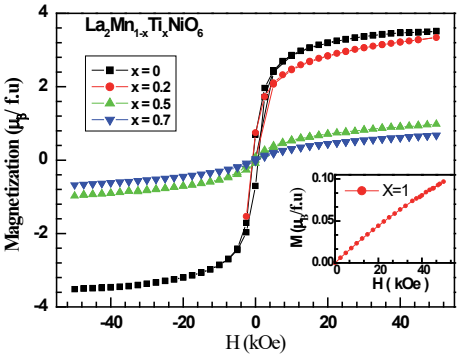

Fig. 3. Isothermal magnetization of $La_2Mn_{1-x}Ti_xNiO_6$ ($x = 0$, 0.2, 0.5 and 0.7) recorded at 5 K. Inset shows the data for La_2TiNiO_6

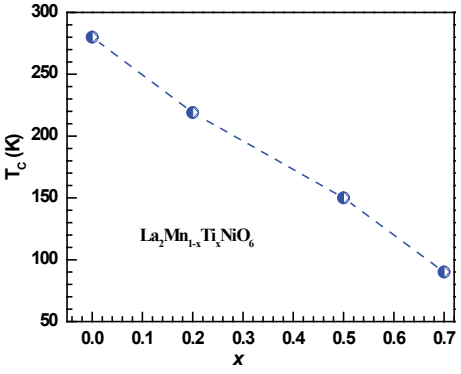

Fig. 4. Variation of ferromagnetic Curie temperature (T_C) with x in $La_2Mn_{1-x}Ti_xNiO_6$

ferromagnetic clusters which are responsible for observed magnetic behaviour of the Ti doped samples even for 70% doping. This is even higher than the effect of Ti doping in spinel structure. $Mn_{1+x}Fe_{2-2x}Ti_xO_4$ has been reported to exhibit ferrimagnetic ordering up to 50% Ti doping [36, 37]. However, one cannot rule out the cationic disordering with the increase in Ti doping. La_2CoTiO_6 and Pr_2CoTiO_6 have been reported to show long-range antiferromagnetism at 15 K and 17 K, respectively, in cationic ordered state. The antiferromagnetic exchange interaction path is $Co^{2+} - O - Ti^{4+} - O - Co^{2+}$ in cationic ordered samples [28, 29]. However, we did not observe any such long range antiferromagnetic ordering in La_2TiNiO_6. The absence of such long range ordering can be related to the cationic disordering.

To look at the magnetic features above T_C we have fitted the high temperature data with Curie-Weiss law. The calculated effective paramagnetic moments also found to decrease with the increase in Ti doping. The μ_{eff} value for the parent phase is 6.30 μ_B/f.u. which is slightly larger than the calculated value 5.97 μ_B/f.u., which has been attributed to the possible formation of ferromagnetic cluster above T_C [38, 39]. The μ_{eff} value decreases from 4.8 μ_B/f.u. for $x = 0.2$ to 1.72 μ_B/f.u. for $x = 1.0$ sample revealing the effect of magnetic dilution. Finally, to confirm the association of low temperature magnetic anomaly with spin glass behaviour as reported for the parent phase we have measured the ac-susceptibility of $x = 0$ and $x = 0.5$ samples at different driving frequencies in the low temperature regions. Fig. 5 shows the real and imaginary parts of the ac-susceptibility data for these two samples. The $\chi'(T)$ for $x = 0$ sample is too broad to uniquely identify the glass transition temperature T_g

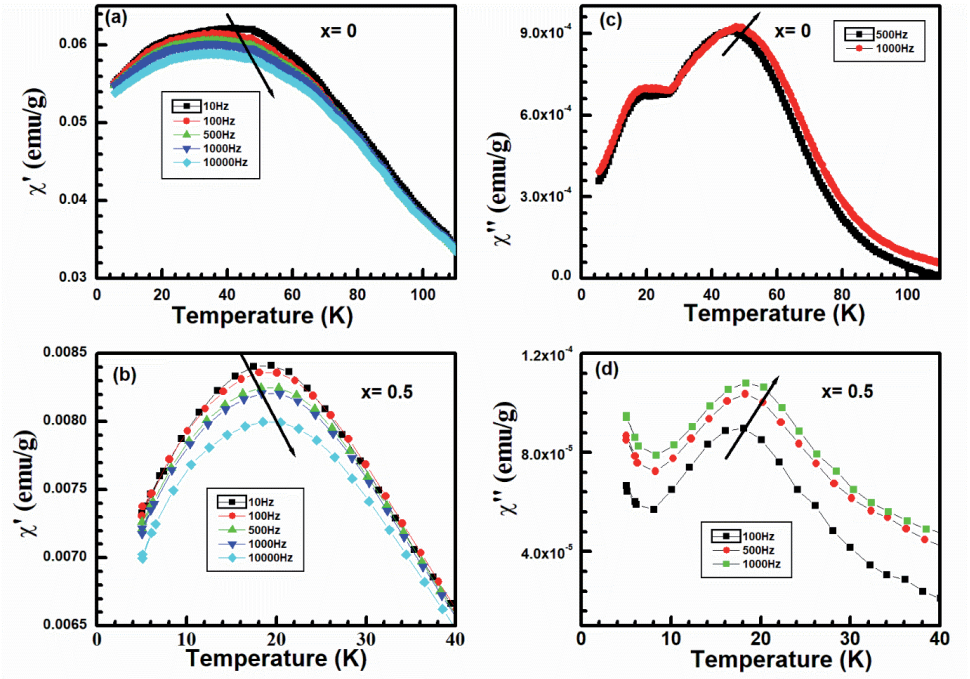

Fig. 5. Temperature dependent ac-susceptibilities of $La_2Mn_{1-x}Ti_xNiO_6$ for $x = 0$ and 0.5. Panels (*a, b*) show real part, $\chi'(T)$, and (*c, d*) show imaginary part, $\chi''(T)$, at selected frequencies

(Fig. 5, *a*). However, the χ"(*T*) revealed two frequency dependent peak around 20 K and 50 K (Fig. 5, *c*), respectively, suggesting the magnetic frustration. The multiglass behaviour of La_2MnNiO_6 has been reported in the literature [18]. This magnetic frustration is associated with the competing interaction between the antisite disorder induced antiferromagnetic $Mn^{4+} - O - Mn^{4+}$ and $Ni^{2+} - O - Ni^{2+}$ interactions and ferromagnetic clusters [18]. The $x = 0.5$ sample exhibit only one peak around 20 K, which is frequency dependent as revealed from both χ'(*T*) and χ"(*T*) data (Figs. 5, *b*, *d*). This indicates the presence of magnetic frustration in pure and Ti doped samples.

Conclusions

In the present study, we have synthesized $La_2Mn_{1-x}Ti_xNiO_6$ ($0 \le x \le 1.0$) by modified citrate-based sol-gel method. Rietveld analysis of the PXRD patterns revealed that the parent phase ($x = 0$) is biphasic in nature composed of rhombohedral $R\bar{3}c$ and monoclinic $P2_1/n$ structures, whereas Ti doped samples crystalized in single phase monoclinic $P2_1/n$ structure with the suppression of rhombohedral phase. The cell volume of the Ti doped samples increased due to larger size of Ti^{4+} compared to Mn^{4+} ion. The magnetic measurements suggest the multiple magnetic transition in La_2MnNiO_6. The high temperature ferromagnetic transition with T_C~280 K associated with the cationic ordered ferromagnetic superexchange interaction $Ni^{2+} - O - Mn^{4+}$ becomes weaker by replacement of Mn^{4+} by nonmagnetic Ti^{4+}. There is a gradual shift in T_C with increase in Ti doping eventually leading to a paramagnetic state in La_2TiNiO_6. The ferromagnetic state of double perovskite exhibits robustness towards Ti substitution compared to the simple perovskite manganite as well as spinels, which may be related to the cationic ordering. Unlike other Ti containing double perovskite, La_2TiNiO_6 fails to show long-range antiferromagnetic ordering probably due to cationic disordering. Both the pure and Ti doped samples show magnetic frustration at lower temperatures.

Acknowledgements

The authors acknowledge the financial support from Indo-Russian project (INT/RUS/RFBR/P-239), Department of Science and Technology (DST), Government of India.

References

1. Raveau B, Seikh Md. M. Cobalt oxides: from crystal chemistry to physics, John Wiley & Sons; 2012.
2. Kobayashi KI, Kimura T, Sawada H, Terakura K, Tokura Y. Room-temperature magnetoresistance in an oxide material with an ordered double-perovskite structure, Nature. Nature. 1998; 395(6703):677–680.
   DOI: 10.1038/27167.
3. von Helmolt R, Wecker J, Holzapfel B, Schultz L, Samwer K. Giant negative magnetoresistance in perovskitelike $La_{2/3}Ba_{1/3}MnO_x$ ferromagnetic films. Phys. Rev. Lett. 1993; 71(14):2331–2333.
   DOI: 10.1103/PhysRevLett.71.2331.

4. Rao CNR, Raveau B. Colossal Magnetoresistance, Charge Ordering and Related Properties of Manganese Oxides,WORLD SCIENTIFIC; 1998.
5. Baettig P, Ederer C, Spaldin NA. First principles study of the multiferroics $BiFeO_3$,Bi_2FeCrO_6 and $BiCrO_6$: Structure, polarization and magnetic ordering temperature. Phys. Rev. B. 2005; 72(21):214105.
DOI: 10.1103/PhysRevB.72.214105.
6. Anderson M, Greenwood K, Taylor G, Poeppelmeier K. B-cation arrangements in double perovskites. Prog. Solid State Chem. 1993; 22(3):197–233.
DOI: 10.1016/0079–6786(93)90004-B.
7. Balcells L, Navarro J, Bibes M, Roig A, Martínez B, Fontcuberta J. Cationic ordering control of magnetization in Sr_2FeMoO_6 double perovskite. Appl. Phys. Lett. 2001; 78(6):781–783.
DOI: 10.1063/1.1346624.
8. Woodward PM. Octahedral Tilting in Perovskites. I. Geometrical Considerations Acta Crystallogr. Sect. B. Struct. Sci. 1997; 53(1):32–43.
DOI: 10.1107/S0108768196010713.
9. Bos J-WG, Attfield JP. Structural and Magnetic Properties of the Double Perovskite $LaCaMnNbO_6$. Z. Anorg. Allg. Chem. 2004; 630(13–14):2248–2252.
DOI: 10.1002/zaac.200400159.
10. Vasala S, Karppinen M. $A_2B'B''O_6$ perovskites: A review. Prog. Solid State Chem. 2015; 43(1–2):1–36.
DOI: 10.1016/j.progsolidstchem.2014.08.001.
11. Ortega N, Kumar A, Scott JF, Katiyar RS. Multifunctional magnetoelectric materials for device applications. J. Phys. Condens. Matter 2015; 27(50):504002.
DOI: 10.1088/0953–8984/27/50/504002.
12. Neenu Lekshmi P, Vasundhara M, Varma MR, Suresh KG, Valant M. Structural, magnetic and dielectric properties of rare earth based double perovskites RE_2NiMnO_6 (RE=La, pr, Sm, Tb). Phys. B Condens. Matter 2014; 448:285–289.
DOI: 10.1016/j.physb.2014.04.057.
13. Yadav R, Nair HS, Kumar A, Adiga S, Bhat HL, Yusuf SM, Elizabeth S. Investigation of dielectric relaxation, Jahn-Teller distortion, and magnetic ordering in Y substituted $Pr_{1-x}Y_xMnO_3(0.1 \leq x \leq 0.4)$. J. Appl. Phys. 2015; 117(9):093903.
DOI: 10.1063/1.4913881.
14. Rogado NS, Li J, Sleight AW, Subramanian MA. Magnetocapacitance and Magnetoresistance Near Room Temperature in a Ferromagnetic Semiconductor: La_2NiMnO_6. Adv. Mater. 2005; 17 (18):2225–2227.
DOI: 10.1002/adma.200500737.
15. Dass RI, Yan, J-Q, Goodenough JB. Oxygen stoichiometry, ferromagnetism, and transport properties of $La_{2-x}NiMnO_{6+\delta}$. Phys. Rev. B 2003; 68(6): 064415.
DOI: 10.1103/PhysRevB.68.064415.
16. Joly VLJ, Joy PA, Date SK, Gopinath CS. Two ferromagnetic phases with different spin states of Mn and Ni in $LaMn_{0.5}Ni_{0.5}O_3$. Phys. Rev. B 2002; 65(18): 184416.
DOI: 10.1103/PhysRevB.65.184416.

17. Biswal AK, Ray J, Babu PD, Siruguri V, Vishwakarma PN. Dielectric relaxations in La_2NiMnO_6 with signatures of Griffiths phase . J. Appl. Phys. 2014; 115(19):194106. DOI: 10.1063/1.4876723.
18. Choudhury D, Mandal P, Mathieu R, Hazarika A, Rajan S, Sundaresan A, Waghmare UV, Knut R, Karis O, Nordblad P, Sarma DD. Near-Room-Temperature Colossal Magnetodielectricity and Multiglass Properties in Partially Disordered La_2MnNiO_6. Phys. Rev. Lett. 127201. doi:10.1103/PhysRevLett.108.127201. 2012;108(12):127201.
19. Mondal P, Bhattacharya D, Choudhury P, Mandal P. Dielectric anomaly at T_N in $LaMnO_3$ as a signature of coupling between spin and orbital degrees of freedom. Phys. Rev. B 2007; 76(17):172403.
DOI: 10.1103/PhysRevB.76.172403.
20. Ricciardo RA, Hauser AJ, Yang FY, Kim H, Lu W, Woodward PM. Structural, magnetic, and electronic characterization of double perovskites $BixLa_{2-x}MnMO_6$ (M = Ni, Co; x = 0.25, 0.50). Mater. Res. Bull. 2009; 44(2):239–247.
DOI: 10.1016/j.materresbull.2008.10.015.
21. Sayed FN, Achary SN, Jayakumar OD, Deshpande SK, Krishna PSR, Chatterjee S, Ayyub P, Tyagi AK. Role of annealing conditions on the ferromagnetic and dielectric properties of La_2NiMnO_6. J. Mater. Res. 2011; 26(4):567–577.
DOI: 10.1557/jmr.2011.4.
22. Gaikwad VM, Yadav KK, Lofland SE, Ramanujachary KV, Chakraverty S, Ganguli AK, Jha M. New low temperature process for stabilization of nanostructured La_2NiMnO_6 and their magnetic properties. J. Magn. Magn. Mater. 2019; 471:8–13.
DOI: 10.1016/j.jmmm.2018.08.081.
23. Biswal AK, Ray J, Babu PD, Siruguri V, Vishwakarma PN. Effect of Cu substitution on the magnetic and dielectric properties of La_2NiMnO_6. J. Appl. Phys. 2015; 117(17):17B728.
DOI: 10.1063/1.4917069.
24. Yuan X, Li Q, Hu J, Xu M. Unusual dynamic magnetic behavior of polycrystalline La_2NiMnO_6. Phys. B Condens. Matter 2013; 424:73–78.
DOI: 10.1016/j.physb.2013.04.057.
25. Chandrasekhar KD, Das AK, Venimadhav A. Spin glass behaviour and extrinsic origin of magnetodielectric effect in non-multiferroic La_2NiMnO_6 nanoparticles. J. Phys. Condens. Matter 2012; 24(37):376003.
DOI: 10.1088/0953–8984/24/37/376003.
26. Dass RI, Goodenough JB. Multiple magnetic phases of $La_2CoMn_{6-\delta}$ ($0<\sim\delta<\sim0.05$). Phys. Rev. B 2003; 67(1):014401.
DOI: 10.1103/PhysRevB.67.01440.
27. Blasse G. Magnetic properties of mixed metal oxides with ordered perovskite structure. Philips Res. Rep. 1965; 20:327.
28. Holman KL, Huang Q, Klimczuk T, Trzebiatowski K, Bos JWG, Morosan E, Lynn JW, Cava RJ. Synthesis and properties of the double perovskites La_2NiVO_6, La_2CoVO_6, and La_2CoTiO_6. J. Solid State Chem. 2007; 180(1):75–83.
DOI: 10.1016/j.jssc.2006.09.013.

29. Das N, Singh R, Das A, Gupta LC, Ganguli AK. Structural, magnetic and dielectric properties of a new double perovskite Pr_2CoTiO_6. J. Solid State Chem. 2017; 253:355–359.
DOI: 10.1016/j.jssc.2017.06.024.
30. Shannon RD. Revised effective ionic radii and systematic studies of interatomic distances in halides and chalcogenides. Acta Crystallogr. Sect. A 1976; 32(5):751–767.
DOI: 10.1107/S0567739476001551.
31. Rodríguez-Carvajal. Recent advances in magnetic structure determination by neutron powder diffraction J. Phys. B Condens. Matter 1993; 192(1–2):55–69.
DOI: 10.1016/0921–4526(93)90108-I.
32. Blasco J, Sánchez MC, Pérez-Cacho J, García J, Subías G, Campo J. Synthesis and structural study of $LaNi_{1-x}Mn_xO_{3+\delta}$ perovskites J. Phys. Chem. Solids 2002; 63(5):781–792.
DOI: 10.1016/S0022-3697(01)00228–1.
33. Azuma M, Takata K, Saito T, Ishiwata S, Shimakawa Y, Takano M. Designed Ferromagnetic, Ferroelectric Bi_2NiMnO_6. J. Am. Chem. Soc. 2005; 127(24):8889–8892.
DOI: 10.1021/ja0512576.
34. Palakkal JP, Sankar CR, Varma MR. Magnetism and magnetoresistance in Al half doped $LaNiO_3$. Mater. Chem. Phys. 2019; 225:316–319.
DOI: 10.1016/j.matchemphys.2019.01.001
35. Sarkar P, Khan N, Pradhan K, Mandal P. Collapse of ferromagnetism with Ti doping in $Sm_{0.55}Sr_{0.45}MnO_3$. Phys. Rev. B 2018; 98(1): 014422.
DOI: 10.1103/PhysRevB.98.014422
36. Mujasambatoo K, Kumar S, Ansari MS. Ferrimagnetic Ordering of Ti^{4+} Doped $Mn_{1+x}Fe_{2-2x}O_4$ ($0 \le x \le 0.5$) Ferrites at Room Temperature. Sci. Adv. Mater. 2011; 3(1):120–126.
DOI: 10.1166/sam.2011.1143
37. Kumar S, Koo BH, Lee CG, Gautam S, Chae KH. Magnetic and Electronic Structure Studies of $Mn_{1+x}Fe_{2-2x}Ti_xO_4$ ($0 \le x \le 0.5$) Ferrites. Funct. Mater. Lett. 2010; 03(04):269–273.
DOI: 10.1142/S1793604710001391.
38. Devi Chandrasekhar K, Das AK, Mitra C, Venimadhav A. The extrinsic origin of the magnetodielectric effect in the double perovskite La_2NiMnO_6. J. Phys. Condens. Matter 2012; 24(49):495901.
DOI: 10.1088/0953–8984/24/49/495901.
39. Zhou S, Shi L, Yang H, Zhao J. Evidence of short-range magnetic ordering above T_C in the double perovskite La_2NiMnO_6. Appl. Phys. Lett. 2007; 91(17):172505.
DOI: 10.1063/1.2801694